Computational Materials Science 114 (2016) 151–159

Contents lists available at ScienceDirect

Computational Materials Science

journal homepage: www.elsevier.com/locate/commatsci

Effects of nonlocal elasticity and slip condition on vibration and stability analysis of viscoelastic cantilever carbon nanotubes conveying fluid

R. Bahaadini, M. Hosseini *

Department of Mechanical Engineering, Sirjan University of Technology, 78137-33385 Sirjan, Islamic Republic of Iran

ARTICLE INFO

Article history:
Received 15 August 2015
Received in revised form 12 December 2015
Accepted 17 December 2015

Keywords:
Cantilever carbon nanotube
Nonlocal elasticity
Structural damping
Knudsen number
Vibration
Stability

ABSTRACT

In this study, effects of nonlocal elasticity and slip condition on free vibration and flutter instability analysis of viscoelastic cantilever carbon nanotubes (CNTs) conveying fluid are investigated. Nonlocal Euler–Bernoulli beam theory is employed to establish the governing equations of motion for the vibrational behavior of CNT. The material property of the CNT is simulated by Kelvin–Voigt viscoelastic constitutive relation. The slip boundary conditions of CNT conveying fluid are considered based on Knudsen number (*Kn*). The equation of motion and associated boundary conditions are derived by using the extended form of Hamilton's principle. The extended Galerkin method is then employed to discretize the equation of motion and boundary conditions which are then solved to calculate the eigenvalues and critical flutter speeds. Detailed results are demonstrated for the dependence of internal moving fluid, nonlocal parameter, structural damping coefficients and Knudsen number on the dimensionless eigenvalues and flutter boundaries of the cantilever CNT. It can be concluded that the structural damping coefficients and Knudsen number does not have a significant effect on the eigenvalues. However, the results show that the structural damping coefficients, Knudsen number and nonlocal parameter have significant effect on the flutter boundaries of the cantilever CNTs.

1. Introduction

Pipes conveying fluid have held wide applications in steam pipes, piping in oil, gas and ocean mining. In particular, the vibrational behavior of a cantilever pipe containing following flow is very different from pipes under other boundary conditions. Because cantilever pipe conveying fluid is a non-conservative system, it loses its stability by flutter (dynamic instability). Hence, cantilever pipe conveying fluid is one of the top subjects which are received great deal of attention by many researchers in the world. Gregory and Païdoussis [1] have been showed that cantilever pipes conveying fluid lose their stability by flutter at sufficiently high flow velocities. Hosseini and Fazelzadeh [2] performed stability analysis of functionally graded cantilever pipe conveying fluid with considering axial end force and thermal field. Yu et al. [3] studied the stability of a periodic cantilever pipe conveying fluid. They used the transfer matrix method to obtain the flutter boundaries of the pipe. Because of the importance of the viscoelastic material properties in the vibration analysis of pipes conveying fluid, several investigations have also considered the flow-induced vibration of viscoelastic macro-scale pipes conveying fluid without size effect [4–7]. They described the effect of the viscoelastic coefficient and mass ratio on the stability boundary and showed that the stability range of the system decreases as viscosity coefficient increases.

Due to the recent technological development in science and engineering, single-walled carbon nanotubes (CNTs) have attracted enormous attention. Extraordinary mechanical properties and potential applications of CNTs have made them suitable for many applications in the fields of chemistry, physics, nanoengineering, electrical engineering, materials science and construction engineering. Therefore, it is crucial to know the mechanical behavior of CNTs such as rotation, elongation and failure [8], buckling and post-buckling [9], vibration [10], thermal vibration [11], and instability analysis [12]. CNTs can be found in many engineering applications for example, as drug delivery [13], micro/nano-electromechanical systems (MEMS/NEMS) [14] and nano pipes containing flowing fluid [15]. Yoon et al. [16] studied the effect of fluid internal flow on free vibrations and flutter instability of cantilevered carbon nanotubes. They applied classical Euler–Bernoulli beam theory to model nanotubes and analyzed its vibrational properties. Wang [17] investigated the vibration and instability of nanotube containing flow using the Eringen nonlocal elasticity theory. He discussed the influence of nonlocal parameter

* Corresponding author. Tel.: +98 34 42 33 69 01; fax: +98 34 42 33 69 00.
E-mail address: hosseini@sirjantech.ac.ir (M. Hosseini).

http://dx.doi.org/10.1016/j.commatsci.2015.12.027
0927-0256/

Nomenclature

Latin symbols

a	internal property of length
A	cross-sectional area
$[\boldsymbol{A}]$	state matrix
b	general slip coefficient
$[\boldsymbol{C}]$	damping matrix
C_{ij}	element of damping matrix
D	outside diameter
e_0	nonlocal material constant
E	elastic modules
E_e	potential energies
g	viscoelastic factor
h	thickness of CNT
i	imaginary unit
I	area moment of inertia of cross-section of CNT
$[\boldsymbol{I}]$	unitary matrix
Kn	Knudsen number
$[\boldsymbol{K}]$	stiffness matrix
K_{ij}	element of stiffness matrix
L	length of CNT
m_f	mass per unit length of fluid
m_c	mass per unit length of the CNT
M	bending moment
$[\boldsymbol{M}]$	mass matrix
M_{ij}	element of mass matrix
N	number of trial functions
q_r	modal coordinates
R_o	outer radius of CNT
t	time
T	dimensionless time
T_t	kinetic energy
u	dimensionless fluid velocity
$u_{avg,slip}$	average fluid speeds through nanotube with slip boundary conditions
$u_{avg,(no\text{-}slip)}$	average fluid speeds through nanotube without slip boundary conditions
u_{cr}	dimensionless critical flutter velocity
U	fluid velocity
w	dimensionless lateral displacement
W	lateral displacement
W^{ext}	work done by non-conservative forces
x	spatial coordinate along the CNT
X	dimensionless spatial coordinate along the CNT
X_1	constant vector
Z	state vector

Greek symbols

α	dimensionless structural damping
β	mass ratio
δ	variation operator
δ_{ij}	Kronecker delta
ε_{xx}	axial strain
λ_c	real part of eigenvalue
μ	nonlocal parameter
ϕ_r	the rth trial function
Ω	imaginary part of eigenvalue
Ω_{cr}	dimensionless critical frequencies
Ω_0	eigenvalue
ρ_c	mass density of nanotube
ρ_w	fluid mass density
σ_v	tangential moment accommodation coefficient
σ_{xx}	axial stress

on the vibrational frequencies. The effect of several parameters such as the radius ratio, transverse shear effect, tube length and van der Waals forces on natural frequency and argand diagram of cantilever multi-wall CNTs conveying fluid was reported in [18] by using nonlocal Euler–Bernoulli and Timoshenko beam theories. Ghavanloo and Fazelzadeh [19] evaluated the vibration equation of a viscoelastic CNTs carrying fluid. They discussed the influence of the nonlocal parameter, external viscous fluid and thermal field to the vibration characteristics of the tube. Wang and Liew [20] studied the vibration and buckling of carbon nanotubes with Eringen's nonlocal elasticity constitutive equations. Also, recent developments in the vibration and stability of CNTs conveying fluid can be pursued in the work of Mirramazani et al. [21], Wang [22,23], Xia and Wang [24], Zhen and Fang [25], Wang and Ni [26] and Ghorbanpour Arani et al. [27].

Recently, the study of small-sized effects of flow field on the vibrational behavior of CNT has received a great deal of attention among researchers. In order to model the nano flow field within the nanotube, a Knudsen number parameter is used. This is a parameter defined as the ratio of the mean free path of the fluid molecules to a characteristic length of the flow. Various value of Knudsen number determines four flow regimes, for example (a) $0 < Kn < 10^{-2}$ for the continuum flow regime, (b) $10^{-2} < Kn < 10^{-1}$ for the slip flow regime, (c) $10^{-1} < Kn < 10$ for the transition flow regime, (d) $10 < Kn$ for the free molecular flow regime. Knudsen number is larger than 10^{-2} for CNTs conveying fluid [28]. The influence of small-sized effects of flow field on the vibration of a nanopipe conveying fluid was studied by Mirramezani and Mirdamadi [29]. They utilized Knudsen number to discretize different flow regimes. Also, they showed the Knudsen number effect on the divergence instabilities of the nano-pipes for pined-pined and clamped-pined boundary conditions. Rashidi et al. [28] revealed that the effect of Knudsen number on the divergence instability of pined-pined CNT conveying liquid and gas fluid flow. Ghorbanpour Arani and Zarei [30] investigated the influence of Knudsen number on eigenvalues of an embedded cantilever CNT conveying nano-magnetic viscous fluid. Also, the effect of the Knudsen number, nonlocal effect and elastic medium on the natural frequency and divergence boundaries of SWCNT conveying fluid were investigated by Hosseini et al. [31]. They analyzed the vibration behavior of SWCNTs conveying fluid for clamped–clamped, clamped-pined and pined-pined boundary conditions. Sadeghi-Goughari and Hosseini [32] presented a modified FSI model regarding the stability and vibration of a SWCNT conveying viscous nanoflow.

Most of studies have investigated the critical flutter speed and stability of classical pipes conveying fluid. Also, some studies have described the vibrational behaviors of the CNTs conveying fluid supported on both ends. On the other hand, there was not any literature describing the influence of the nonlocal parameter, structural damping coefficients and Knudsen number on the flutter boundary and stability region of the cantilever CNTs conveying fluid. The present paper is aimed to study the vibration and flutter instability of viscoelastic cantilever CNT conveying fluid. The viscoelastic property is considered as a Kelvin-type model, and internal moving fluid is characterized by two parameters, the modified flow velocity ($VCF \times U$) and the mass density of fluid (m_f). The equation of motion and boundary conditions are derived via extended Hamilton's principle. Then, the partial differential equations of motion converted into coupled sets of ordinary differential equations by applying the extended Galerkin method and are then

used for stability analysis of the system. After that, the influence of different physically parameters, including the nonlocal parameter, structural damping coefficients, Knudsen number and mass ratio on the both vibrational frequency and flutter instability of the system are investigated. The variations in critical flutter speed of a viscoelastic CNT conveying fluid can specifically affect on the structural design of nano-mechanical systems conveying fluid includes nanofluidics and nanobiological devices. Therefore an accurate and general modeling of these systems is important for their design and analysis.

2. Governing equations and boundary conditions

Fig. 1 demonstrates viscoelastic cantilever CNT of length L, outside diameter D, cross-sectional area A with bending rigid body of EI. Its mass per unit length of the CNT, mass per unit length of fluid and the velocity of fluid are m_c, m_f and U, respectively. Let $w(x, t)$ be the lateral displacement, x is the spatial coordinate along the CNT, and t is the time. It is assumed that gravity effects and the externally imposed tension and pressure are disregarded in CNT.

According to Païdoussis [33], the equation of motion and boundary condition can be driven from extended Hamilton principle for an open-system characterized with input and output mass and momentum. Therefore it is formulated as follow:

$$\delta\int_{t1}^{t_2}\left(T_t - E_e + W^{ext} - \frac{1}{2}m_f U^2\int_0^L\left(\frac{\partial w}{\partial x}\right)^2\right)dt - \int_{t1}^{t_2} m_f U\left(\frac{\partial w_L}{\partial t} + U\frac{\partial w_L}{\partial x}\right)\delta w_L = 0 \quad (1)$$

where T_t and E_e denote kinetic energy of system and potential energies, respectively and W^{ext} is the work done by non-conservative forces. Also, δ is the variation operator. Moreover, $(.)_L$ denotes the values of the corresponding quantities (.) at $x = L$.

For CNTs conveying fluid, Knudsen number is larger than 10^{-2}. Therefore, the assumption of no-slip boundary conditions is no longer credible, and a modified model should be used. Rashidi et al. [28] utilized a modified nanotube that includes nano-flow viscosity and slip boundary condition. They replaced U by $u_{avg,slip} = VCF \times u_{avg,(no\text{-}slip)}$ in the equation of motion. Where $u_{avg,slip}$ and $u_{avg,(no\text{-}slip)}$ are the average fluid speeds through nanotube with slip boundary conditions and without slip boundary conditions, respectively. Also, VCF is the average velocity correction factor which can be assumed as [28]:

$$VCF = \frac{u_{avg,slip}}{u_{avg,(no-slip)}} = (1 + a_k Kn)\left(4\left(\frac{2-\sigma_v}{\sigma_v}\right)\left(\frac{Kn}{1+Kn}\right) + 1\right) \quad (2)$$

where Kn is Knudsen number, σ_v is tangential moment accommodation coefficient which is considered to be 0.7 for most practical purposes [28]. Furthermore, a_k is a coefficient which can be derived as [34]:

$$a_k = a_0\frac{2}{\pi}\left[\tan^{-1}(a_1 Kn^B)\right] \quad (3)$$

The values of $a_1 = 4$ and $B = 0.4$ are some empirical parameters and a_0 is a coefficient, as follow [34]:

$$a_0 = \frac{64}{3\pi(1 - 4/b)} \quad (4)$$

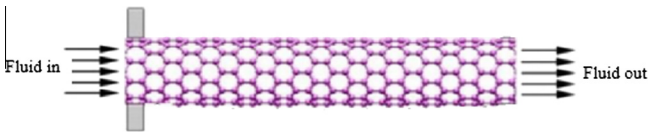

Fig. 1. Schematic of a cantilevered CNT conveying fluid.

where $b = -1$ is the general slip coefficient.

Based on the above-mentioned understanding, the first variational of kinetic energy of CNT and fluid flow is given as below:

$$\delta T_t = -m_c\int_0^L\frac{\partial w}{\partial t}\frac{\partial \delta w}{\partial t}dx + m_f\int_0^L\left[\frac{\partial w}{\partial t}\frac{\partial \delta w}{\partial t} + u_{avg,slip}\frac{\partial w}{\partial t}\frac{\partial \delta w}{\partial x} + u_{avg,slip}\frac{\partial w}{\partial x}\frac{\partial \delta w}{\partial t}\right]dx \quad (5)$$

In addition, changes in strain energy for one-dimensional vibrations of nanotubes following linear Hooke's law at the nano-scale of nonlocal elasticity theory are expressed as follow:

$$\delta E_e = \int_0^L\int\int_A \sigma_{xx}\delta\varepsilon_{xx}dAdx \quad (6)$$

where σ_{xx} and ε_{xx} represent nonlocal axial stress and strain in x direction, respectively. The small deflection Euler–Bernoulli relation between strain and curvature is

$$\varepsilon_{xx} = -z\frac{\partial^2 w}{\partial x^2} \quad (7)$$

where z is the distance from the reference point to the middle plane of the CNT's cross section. By substituting Eqs. (7) in (6) and then, making standard manipulations with part-by-part integration of terms, one obtains:

$$\delta E_e = -\int_0^L\frac{\partial^2 M}{\partial x^2}\delta w dx - M\frac{\partial \delta w}{\partial x}\Big|_0^L + \frac{\partial M}{\partial x}\delta w\Big|_0^L \quad (8)$$

where M is the resultant bending moment, which can be expressed as $M = \int\int \sigma_x z dA$.

On the other hand, from nonlocal theory of linear elasticity in the one-dimensional case for homogeneous and isotropic nanotubes, functional equation is expressed as follows.

$$\sigma_{xx} - (e_0 a)^2\frac{\partial^2\sigma_{xx}}{\partial x^2} = E\varepsilon_{xx} \quad (9)$$

where e_0 is a material constant and a is internal property of length. Therefore, $e_0 a$ displays the nonlocal parameter that incorporates the small scale effects into the constitutive equations for free vibration and dynamic structural instability. Based on Kelvin–Vogit model, for elastic materials with viscoelastic factor g, elastic modules E should be substituted by $E(1 + g\frac{\partial}{\partial t})$ [35] then functional equation can be written as follow:

$$\sigma_{xx} - (e_0 a)^2\frac{\partial^2\sigma_{xx}}{\partial x^2} = E\varepsilon_{xx} + g\frac{\partial\varepsilon_{xx}}{\partial t} \quad (10)$$

Multiplying both right and left hands of above equation by z and performing integrating over the nanotube cross-section, it will be as follow:

$$\frac{\partial^2 M}{\partial x^2} = \frac{1}{(e_0 a)^2}\left[M + EI\frac{\partial^2 w}{\partial x^2} + gI\frac{\partial^3 w}{\partial x^2\partial t}\right] \quad (11)$$

Substituting Eqs. (5) and (8) in Eq. (1) and taking integration by parts and noticing that for every admissible variation, the coefficient of this variation must be zero, one may find that the governing equation of motion is obtained as

$$2m_f(VCF \times u_{ave,no-slip})\frac{\partial^2 w}{\partial x\partial t} + m_f(VCF \times u_{avg,no-slip})^2\frac{\partial^2 w}{\partial x^2} + (m_c + m_f)\frac{\partial^2 w}{\partial t^2} - \frac{\partial^2 M}{\partial x^2} = 0 \quad (12)$$

Substituting Eqs. (11) in (12), taking differentiation twice with respect to x and again using Eq. (12), the governing differential equation of motion and boundary conditions of nonlocal CNT conveying flow can be expressed as

$$gI\frac{\partial^5 w}{\partial x^4\partial t}+EI\frac{\partial^4 w}{\partial x^4}+2m_f\left(VCF\times u_{avg,no-slip}\right)\frac{\partial^2 w}{\partial x\partial t}+m_f\left(VCF\times u_{avg,no-slip}\right)\frac{\partial^2 w}{\partial x^2}+(m_c+m_f)\frac{\partial^2 w}{\partial t^2}-(e_0a)^2\left[2m_f\left(VCF\times u_{avg,no-slip}\right)\frac{\partial^4 w}{\partial x^3\partial t}+m_f\left(VCF\times u_{avg,no-slip}\right)^2\frac{\partial^4 w}{\partial x^4}+(m_c+m_f)\frac{\partial^4 w}{\partial x^2\partial t^2}\right]=0 \tag{13}$$

at $x = 0$

$$w=\frac{\partial w}{\partial x}=0 \tag{14}$$

at $x = L$

$$-gI\frac{\partial^3 w_L}{\partial x^2\partial t}-EI\frac{\partial^2 w_L}{\partial x^2}+(e_0a)^2\left[2m_f\frac{\partial^2 w_L}{\partial x\partial t}+m_f\left(VCF\times u_{avg,no-slip}\right)\frac{\partial^2 w_L}{\partial x^2}+(m_c+m_f)\frac{\partial^2 w_L}{\partial t^2}\right]=0$$
$$-EI\frac{\partial^3 w_L}{\partial x^3}+(e_0a)^2\left[2m_f\left(VCF\times u_{avg,no-slip}\right)\frac{\partial^3 w_L}{\partial x^2\partial t}+m_f\left(VCF\times u_{avg,no-slip}\right)^2\frac{\partial^3 w_L}{\partial x^3}+(m_c+m_f)\frac{\partial^3 w}{\partial x^2\partial t}\right]=0 \tag{15}$$

3. Solution procedure

In order to simplify the analysis, the following dimensionless quantities are defined:

$$W=\frac{w}{L}\ X=\frac{x}{L}\ u=\left(\frac{m_f}{EI}\right)^{1/2}Lu_{avg,no-slip}\ \beta=\frac{m_f}{m_f+m_c}$$
$$\mu=\frac{e_0a}{L}\ T=\frac{t}{L^2}\left(\frac{EI}{m_f+m_c}\right)^{1/2}\ \alpha=\frac{g}{EL^2}\left(\frac{EI}{m_c+m_f}\right)^{1/2} \tag{16}$$

3.1. Galerkin approach

Extended Galerkin method is one of the few invaluable methods which is employed to approximate the partial differential equations of motion and associated boundary conditions by a finite dimensional system of coupled ordinary differential equations. This method uses the representation of the unknown displacements in the form of linear combination of trial functions that satisfies the appropriate boundary conditions. According to this method, the function w is approximated as

$$W(X,T)=\sum_{r=1}^{N}q_r(T)\phi_r(X) \tag{17}$$

where N is the number of modes and $q_r(T)$ represents r th modal coordinates. For a cantilever CNT, orthogonal function is as [2]:

$$\phi_r(X)=\cosh\lambda_rX-\cos\lambda_rX-\sigma_r(\sinh\lambda_rX-\sin\lambda_rX)$$
$$\sigma_r=\frac{\sinh\lambda_r-\sin\lambda_r}{\cosh\lambda_r-\cos\lambda_r} \tag{18}$$

and λ_r is the rth dimensionless eigenvalue of the rth flexural mode $\phi_r(X)$ which can be obtained from the following equation:

$$\cosh(\lambda_r)\cos(\lambda_r)+1=0 \tag{19}$$

Applying the extended Galerkin procedure, a set of coupled ordinary-differential equations is obtained as:

$$[\mathbf{M}]\{\ddot{\mathbf{q}}(T)\}+[\mathbf{C}]\{\dot{\mathbf{q}}(T)\}+[\mathbf{K}]\{\mathbf{q}(T)\}=0 \tag{20}$$

where $\mathbf{q}(T)$ is the overall vector of generalized coordinates and the dot notation refers to derivative with respect to time. Also, [**M**], [**C**] and [**K**] are the mass, damping and stiffness matrices, respectively, with the following elements

$$M_{ij}=\delta_{ij}-\mu^2\vartheta_{ij},$$
$$C_{ij}=\alpha\zeta_{ij}+2\beta^{1/2}(VCF\times u)\xi_{ij}-2\mu^2(VCF\times u)\beta^{1/2}\upsilon_{ij}$$
$$K_{ij}=\zeta_{ij}+(VCF\times u)^2\varsigma_{ij}-\mu^2\left[(VCF\times u)^2\zeta_{ij}\right] \tag{21}$$

where

$$\delta_{ij}=\begin{cases}1 & i=j\\ 0 & i\neq j\end{cases}$$
$$\vartheta_{ij}=\begin{cases}\sigma_i\lambda_i(2+\sigma_i\lambda_i) & i=j\\ 4\frac{\lambda_i\lambda_j}{\lambda_i^2-\lambda_j^2}\left((-1)^{i+j}\left(\sigma_j\lambda_i^3-\sigma_i\lambda_j^3\right)-\lambda_i\lambda_j(\sigma_i\lambda_i-\sigma_j\lambda_j)\right) & i\neq j\end{cases}$$
$$\zeta_{ij}=\begin{cases}\lambda_i^4 & i=j\\ 0 & i\neq j\end{cases}$$
$$\xi_{ij}=\begin{cases}2 & i=j\\ 4\frac{\lambda_j^2}{\lambda_i^4-\lambda_j^4}\left(\lambda_i^2-(-1)^{i+j}\lambda_j^2\right) & i\neq j\end{cases}$$
$$\varsigma_{ij}=\begin{cases}\sigma_i\lambda_i(2-\sigma_i\lambda_i) & i=j\\ 4\frac{\lambda_j^2(\sigma_i\lambda_i-\sigma_j\lambda_j)}{\lambda_i^4-\lambda_j^4}((-1)^{i+j}\lambda_j^2+\lambda_i^2)) & i\neq j\end{cases} \tag{22}$$
$$\upsilon_{ij}=\begin{cases}-2\sigma_i^2\lambda_i^2 & i=j\\ 4\frac{\lambda_j^3\lambda_i\sigma_j\lambda_j}{\lambda_i^4-\lambda_j^4}((-1)^{i+j}\lambda_j^2+\lambda_i^2)) & i\neq j\end{cases}$$

3.2. Stability analysis

For the stability analysis, the Eq. (20) is defined into the first order state-space form:

$$\dot{\mathbf{Z}}(T)=[\mathbf{A}]\mathbf{Z}(T) \tag{23}$$

where the state vector $\mathbf{Z}(T)$ is define as

$$\mathbf{Z}(T)=\begin{Bmatrix}\mathbf{q}(T)\\ \dot{\mathbf{q}}(T)\end{Bmatrix} \tag{24}$$

and the $2N \times 2N$ state matrix [**A**] has the form

$$[\mathbf{A}]=\begin{bmatrix}[0] & [\mathbf{I}]\\ -[\mathbf{M}]^{-1}[\mathbf{K}] & -[\mathbf{M}]^{-1}[\mathbf{C}]\end{bmatrix} \tag{25}$$

while [**I**] is the unitary matrix. The solution of Eq. (23) has an exponential form as

$$\mathbf{Z}(t)=\mathbf{X}_1\exp(\Omega_0t) \tag{26}$$

Substituting Eqs. (26) in (23) leads to a standard eigenvalue problem in the form

$$([\mathbf{A}]-\Omega_0[\mathbf{I}])\mathbf{X}_1=0 \tag{27}$$

In which Ω_0 is eigenvalue and $\mathbf{X}_1$ represents its corresponding eigenvector. Since matric [**K**] is asymmetrical, hence the eigenvalue in general manner is a complex value as $\Omega_0=\lambda_c\pm i\Omega$. It should be noted that λ_c and Ω are real and imaginary parts of eigenvalue Ω_0 where the former is called modal damping and latter serves as frequency in proportion to system vibrations frequency. To have a nontrivial solution for the Eq. (27), the determinant of the coefficient matrix must be equal to zero, that is:

$$\det([\mathbf{A}]-\Omega_0[\mathbf{I}])=0 \tag{28}$$

Expansion of the determinant of the above equation provides the system characteristic equation. So the system is stable if and only if all eigenvalues of matrix [**A**] have negative real parts ($\lambda_c<0$) and unstable if at least one eigenvalue has a positive real component ($\lambda_c>0$). When real part of the eigenvalue changes its

sign from negative to positive, $\lambda_c = 0$, two important type of instability occurs. If $\Omega \neq 0$, the system loses stability by flutter. Whenever for $\Omega = 0$, the system loses stability by divergence.

4. Numerical results and discussion

In this section, numerical vibration and flutter instability analysis of the viscoelastic CNTs conveying fluid are investigated. In the following calculations, the values for several physical parameters of the CNT and fluid are displayed in Table 1. Also, the dimensional nonlocal parameter μ, structural damping coefficients α, and Knudsen number Kn are chosen to vary from 0 to 0.2, 0 to 0.1, and 0 to 0.1, respectively.

4.1. Method of solution and Model independency

According to the mathematical description given in the previous sections, a computer program (Matlab) is designed to perform the vibration and stability analysis of the problem. During the discretization, the expansion series given by Eq. (17) were truncated. Therefore, it is important to ensure the convergence of the method for an accurate solution. So, a convergence study was performed in Table 2 to determine the non-dimensional eigenfrequencies and critical flutter velocities of cantilevered CNT conveying fluid with consideration of structural damping and Kn. For a fixed number of trial functions retained at N, the eigenvalues solution is performed for a CNT with $\beta = 0.5$, $\mu = 0.1$, $\alpha = 0.001$ and $Kn = 0.1$. The value of N was increased and the eigenvalues were again computed. It is seen that once a sufficient number of trial functions is used, the first two eigenvalues and critical flutter speed of the CNT does not change significantly. Increasing the number of trial functions further reduces the relative error but increases the computational time. Clearly, a minimum number of trial functions are desired for reducing the computational time while achieving accurate results. Thus, eight number of trial functions can be used for achieving a solution with relative error of less than 0.1% for eigenfrequencies, and less than 0.4% for critical flutter speed. In the next section, the effects of the main parameters including the fluid velocity, mass ratio, small-scale size, structural damping coefficients and Knudsen number on eigenvalues and flutter instability of the CNTs conveying fluid were also studied.

Table 1
Values for physical parameters of CNT [36].

Physical properties and parameters	Values
Elastic modulus, E(TPa)	3.4
CNT density, ρ_c(kg/m^3)	2300
Outer diameter, R_o(nm)	3
Thickness, h(nm)	1
Length, L(nm)	300
Fluid density, ρ_w(kg/m^3)	1000

Table 2
Convergence and accuracy of the first two eigenvalues and critical flutter velocity for cantilevered CNT conveying fluid for various numbers of trial functions (N), ($\beta = 0.5$, $\mu = 0.1$, $\alpha = 0.001$ and $Kn = 0.1$).

N	Mode sequences		u_{cr}
	1st	2nd	
3	−2.59926 + 2.74545i	−2.58693 + 19.44375i	3.834
4	−2.59828 + 2.74375i	−2.51050 + 19.40352i	3.755
5	−2.59587 + 2.73805i	−2.49653 + 19.39420i	3.637
6	−2.59491 + 2.73630i	−2.48135 + 19.38050i	3.587
7	−2.59401 + 2.73383i	−2.47504 + 19.37460i	3.581
8	−2.59343 + 2.73261i	−2.46925 + 19.36725i	3.567
9	−2.59295 + 2.73122i	−2.46602 + 19.36294i	3.563
10	−2.59257 + 2.73037i	−2.46315 + 19.35826i	3.556

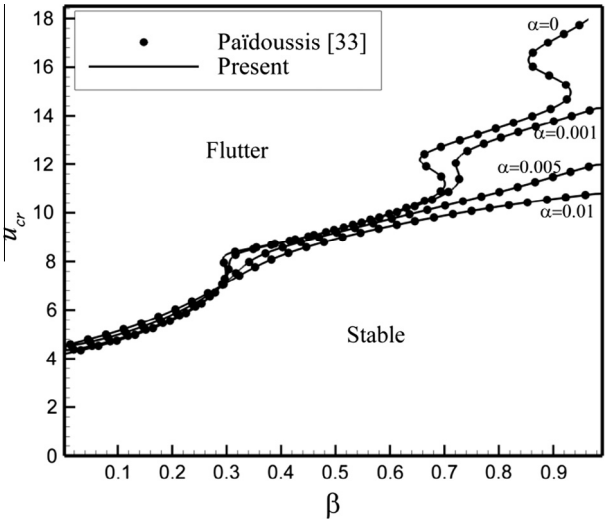

Fig. 2. Validation of the flutter instability boundary of cantilever pipe conveying fluid for $\mu = Kn = 0$.

4.2. Validation of the model

In this section, a numerical study has been conducted to investigate eigenvalues and flutter instability of a cantilever CNT conveying fluid. In order to validate the proposed model, the results are shown only for cantilever pipes conveying fluid, regardless of the slip boundary conditions of nano-flow passing over the CNT walls and the effects of small-scale parameter. It can be seen that the results have a good agreement with the results presented by Païdoussis [33] and Ni et al. [37] in Figs. 2 and 3, respectively.

4.3. Effects of several parameters on the vibration and stability of CNT

4.3.1. Vibration analysis

In this subsection, a numerical study is carried out to investigate the vibration behavior of the CNT conveying fluid by considering the effects of structural damping, nonlocal parameter and Knudsen number (Kn). The effect of moving fluid speed u and structural damping α on variation of the lowest eigenvalues of the cantilever CNT with $Kn = 0$, $\mu = 0$ and $\beta = 0.5$ is plotted in Fig. 4. It is obvious that the structural damping is not a significant parameter in evaluating of the first eigenvalue over the whole range of fluid velocity. Also, the imaginary part (Ω) of eigenvalue becomes zero when $u \cong 3.1$ and real part (λ_c) is divided into two branches. In other words, bifurcation of first eigenvalue solution occurs at this point. These two branches merge again into single one at $u \cong 5.5$. Therefore, when fluid velocity varies in the range between $u \cong 3.1$ and $u \cong 5.5$, over damping mode of the system is resulted and CNT does not vibrate. Also, the imaginary part of eigenvalue increases in magnitude as fluid flow speed increases after $u \cong 5.5$. As indicated in Fig. 4, the real part of eigenvalue is kept negative in the evolution as fluid flow speed increases. Thus, the first mode is always kept stable.

Other parameters which were considered in this study are nonlocal parameter and Knudsen number. Knudsen number is defined based on the various flow regimes. Here, slip flow regime is considered. Fig. 5a and b, respectively, show real and imaginary components of eigenvalues in terms of flow velocity for $Kn = 0.1$, $\alpha = 10^{-3}$ and different amounts of nonlocal parameter. In the mentioned figure, two modes of vibration system are shown.

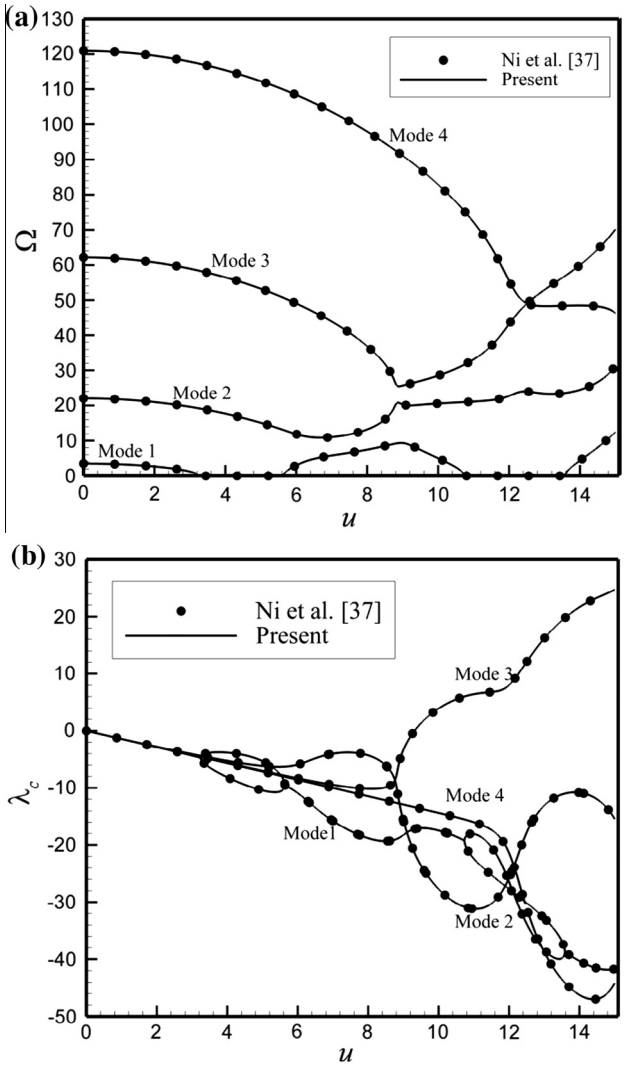

Fig. 3. Validation of the four first eigenvalues of cantilever pipe conveying fluid ($\beta = 0.5$, $\mu = \alpha = Kn = 0$), (a) imaginary part and (b) real part.

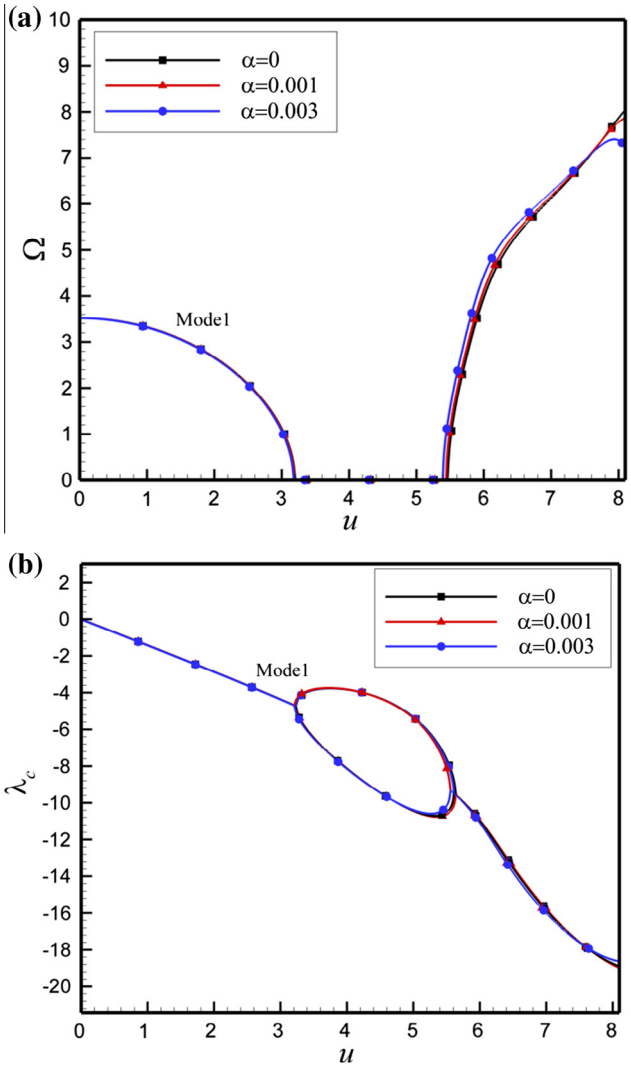

Fig. 4. Variation of first eigenvalue with dimensionless fluid velocity for various structural damping ($\mu = Kn = 0$), (a) imaginary part and (b) real part.

It can be seen that by increasing nonlocal parameter, natural frequency for both modes decreases. So the second natural frequency decreases more when compared to its first natural frequency. Results indicate that with increasing nonlocal parameter, the bifurcation point for the real parts of the first eigenvalue occurs at lower speeds. Therefore, with considering nonlocal parameter and Knudsen number, over damping in CNT occurs in lower fluid velocity. As shown, the second mode becomes unstable by flutter instability at $u \cong 5.1$ when $\mu = 0.1$, $Kn = 0.1$ and $\beta = 0.5$. However, a jump occurs at $u \cong 5.56$. After that point, with the increasing of fluid velocity, real part of eigenvalue will be negative until fluid velocity reaches to $u \cong 7$. This means that system loses its stability in the range of u between 5.1 and 5.56. Then CNT gain its stability when fluid velocity is in the range of $5.56 < u < 7$. For fluid velocity more than $u \cong 7$, system loses its stability again by flutter.

4.3.2. Stability analysis

In this subsection, the stability region and prediction of the critical flutter speed are the core of discussion. Cantilever CNT carrying fluid is a non-conservative system and loses its stability via flutter at $u = u_{cr}$. Critical flutter speed occurs when the real part of the eigenvalue changes its sign from negative to positive and the imaginary part of the eigenvalue is not zero. In this subsection, the effects of mass ratio, nonlocal parameter, structural damping and Kn on the flutter instability of CNTs conveying fluid are investigated.

Fig. 6a and b, respectively, show critical speed and corresponding critical frequency for flutter of cantilever CNT containing fluid flow versus mass ratio for $\mu = 0.05$, $Kn = 0$ and different values of structural damping $\left(\alpha = 0, 10^{-3}, 10^{-2}, 10^{-1}\right)$. These curves that separate the stable area from unstable area are called flutter instability boundary. At speeds below the flutter speed, the vibrational motion will eventually decay regardless of the initial conditions, whereas at speeds above the flutter speed any initial dynamic structural disturbance will grow until strains become high enough for catastrophic structural failure to occur. In Fig. 6a for the special range of β lower than 0.28, it can be observed that non-dimensional critical speed increases when the structural damping increases. In the other hand, for $0.28 < \beta < 1$, u_{cr} decreases with increasing structural damping. Therefore, dissipative forces have stabilizing effect for low value of mass ratio. While the influence of damping causes the CNT to become less stable for high value of mass ratio. It is well known that the critical flutter speed of dynamic instability depends on the energy balance between energy input due to negative work of the fluid velocity, the stored energy by the elastic component and energy dissipation by viscous

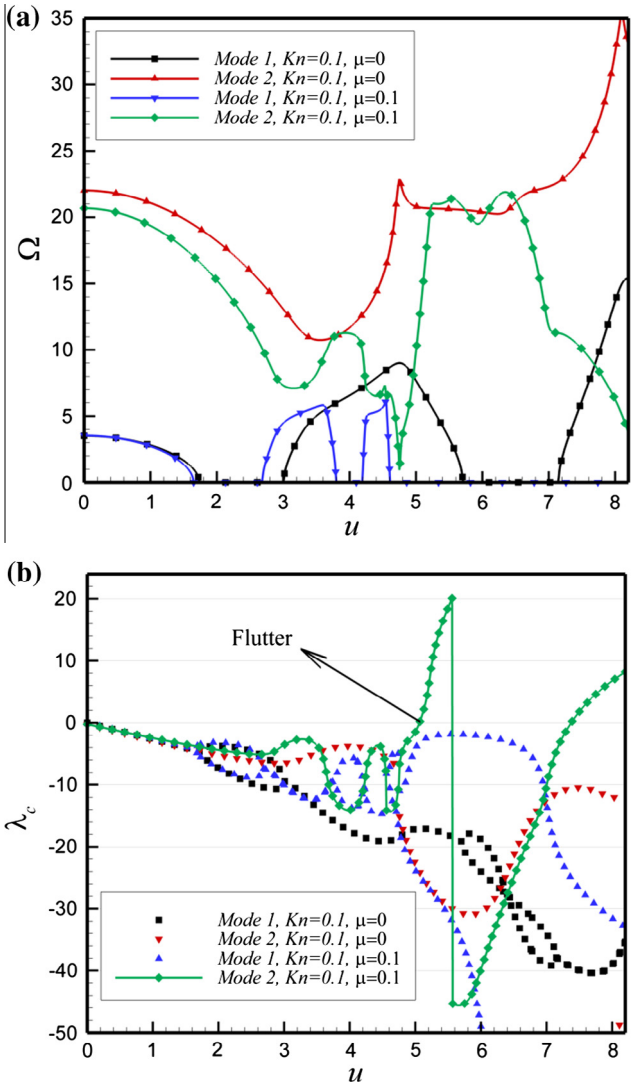

Fig. 5. Variation of two first eigenvalues with dimensionless fluid velocity for two values of nonlocal parameter ($Kn = 0.1$, $\alpha = 10^{-3}$, $\beta = 0.5$), (a) imaginary part and (b) real part.

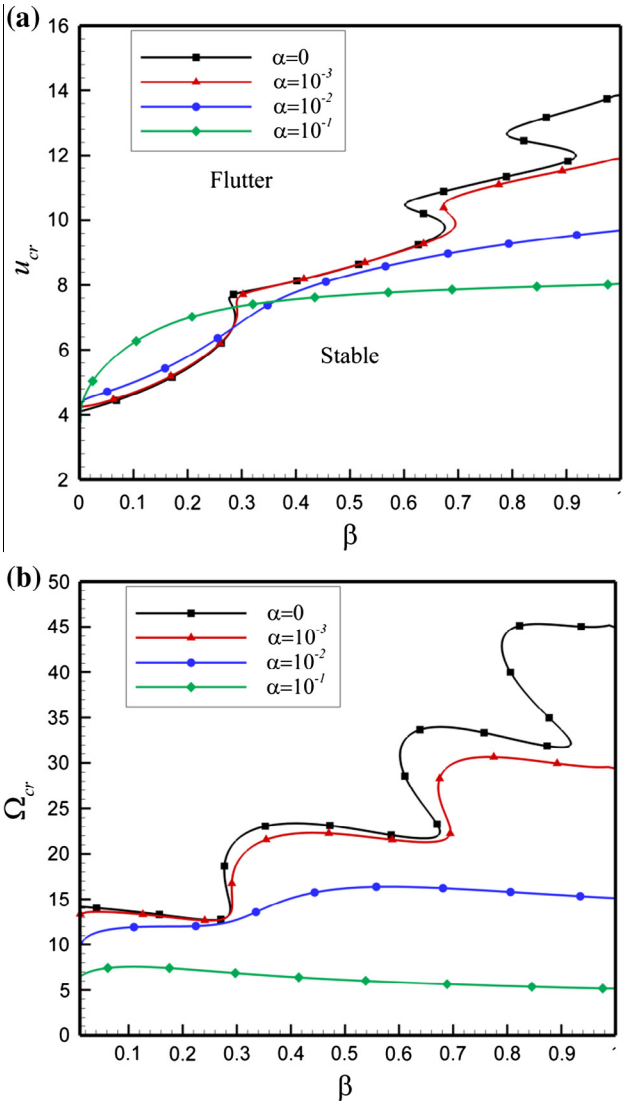

Fig. 6. Flutter boundary in terms of mass ratio for various value of structural damping ($\mu = 0.05$, $Kn = 0$), (a) u_{cr}, and (b) Ω_{cr}.

component of the viscoelastic CNT. Further, it can be also observed that the flutter boundaries for low value of structural damping have several S-shaped segments. In which, by increasing structural damping, the number of S-shaped segments are reduced. Every S-shaped segment represents instability-restabilitization-instability sequence. Also, for the higher value of structural damping, the lower rate of growth of non-dimensional critical speed is observed with respect to mass ratio.

Fig. 6b demonstrates that the higher value of structural damping leads to the lower rate of growth of non-dimensional critical frequency with respect to mass ratio. Also, by increasing structural damping, non-dimensional critical frequency decreases for all range of mass ratio β. This fact physically implies that the frequency becomes smaller due to the increase of energy dissipation.

As the sized scale of CNTs is sufficiently small, the classical local elastic models may be no longer accurate enough and cannot predict the behavior of nanoscale materials anymore. Nonlocal continuum mechanics regards size dependence and small-scale effects in the elastic solutions of nanostructures, and consider forces between atoms and internal length scale in the construction of constitutive equations. Therefore, the nonlocal elasticity theories represent a more accurate mechanical model on the nanoscale structure. In order to study the small- scale effect on the flutter boundaries of a cantilever CNT conveying fluid Fig. 7 is used. In Fig. 7a the critical speed are drawn as a function of nonlocal parameters for different values of mass ratio. In this figure, $\alpha = 0.001$ and $Kn = 0.1$ are assumed. We expect that increasing in nonlocal parameter leads to decreasing of critical speed in flutter conditions. Also, it can be seen that with increasing in mass ratio, no tangible changes will be made in higher values of nonlocal parameter. Thus, CNT flutters under very low speeds for low mass ratio and large nonlocal parameter. Fig. 7b shows stability curves in the $\mu - u_{cr}$ plane for $\beta = 0.1$, $Kn = 0$ and for different values of α. It can be seen from this figure, the dimensionless critical speed decreases when nonlocal parameter increases that indicates a reduction of the stability region. It means that by increasing nonlocal parameter, interaction force between nanotube atoms decreases, and makes CNT more flexible than classical one. Also, by increasing the structural damping, critical speed increases for $\beta = 0.1$. Therefore, one can recognize that nonlocal parameter decreases the critical speed regardless of existence of structural damping.

In order to evaluate the effects of the Knudsen number parameter on the stability boundary of CNT, the changes in critical flow

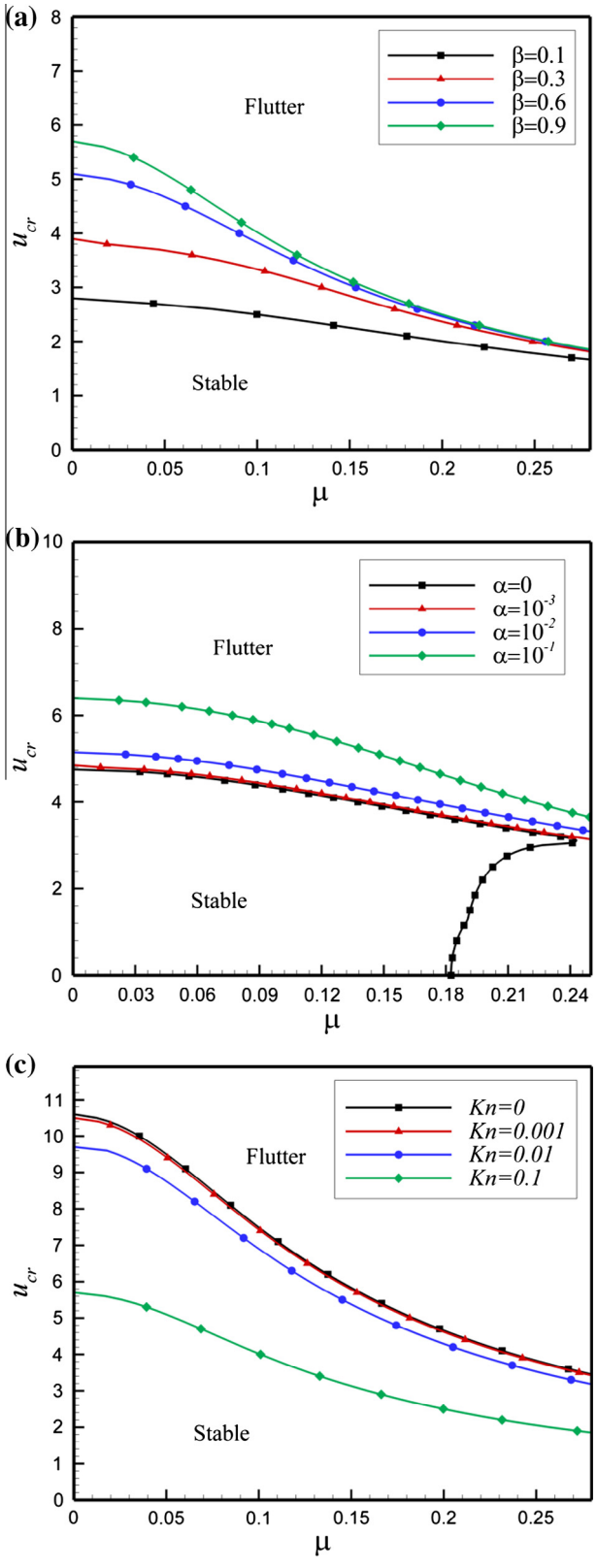

Fig. 7. Flutter boundary in terms of nonlocal parameter for various values of (a) β ($\alpha = 0.001$, $Kn = 0.1$), (b) Kn ($\alpha = 0.01$, $\beta = 0.9$), and (c) α ($\beta = 0.1$, $Kn = 0$).

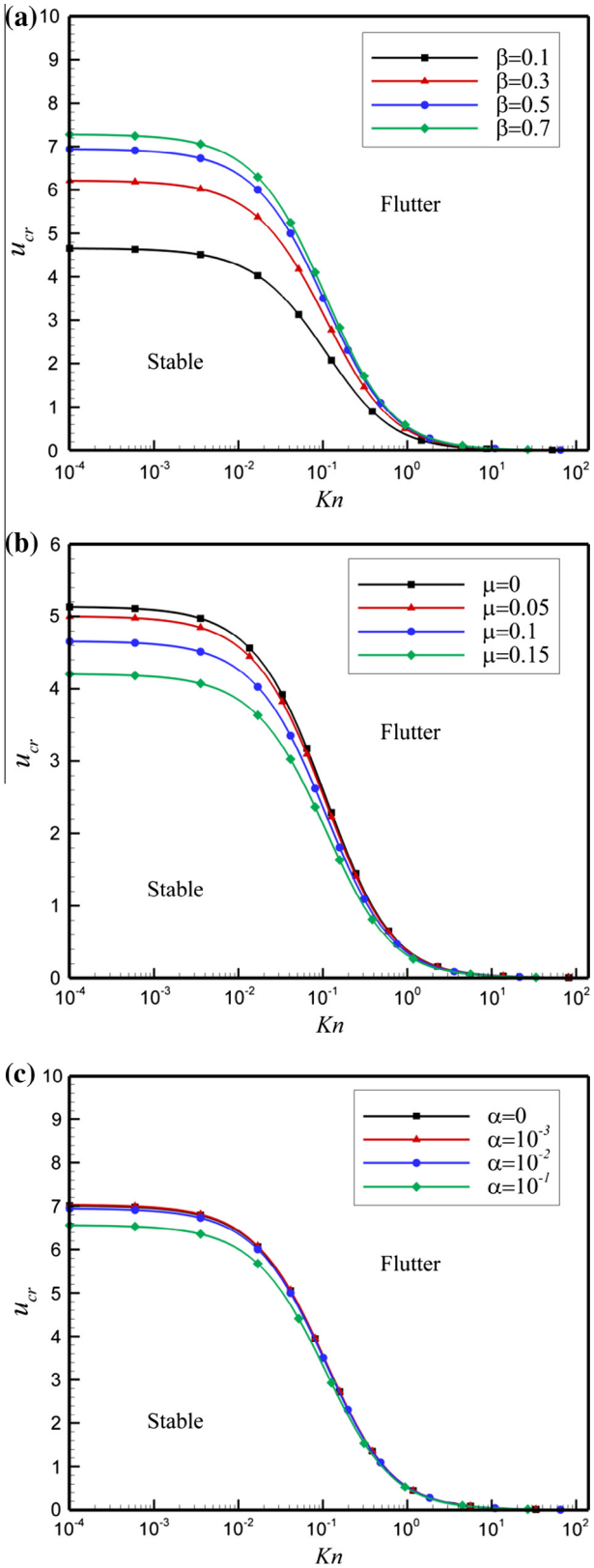

Fig. 8. Flutter boundary curves vs. Knudsen parameter for various values of (a) β ($\mu = 0.1$, $\alpha = 0.01$), (b) μ ($\beta = 0.1$, $\alpha = 0.01$), and (c) α ($\beta = 0.5$, $\mu = 0.1$).

rate are drawn in Fig. 7c as a function of nonlocal parameter for different values of Knudsen parameters ($Kn = 0, 0.001, 0.01, 0.1$), with $\beta = 0.9$ and $\alpha = 0.01$. It can be seen that by increasing the Knudsen parameter, the critical flow velocity reduces. In other words, when the ratio of mean free path of the fluid molecules is greater than the length of flow property, the stability region of CNT will be decreased.

Fig. 8 illustrate the variation of critical flow velocity (u_{cr}) against Knudsen number, while the effects of other parameters, i.e., mass ratio, nonlocal parameter and structural damping are examined. The Knudsen number is considered varying from $Kn = 10^{-4}$ to 10^{2} with logarithmic scale on the horizontal axis.

Fig. 8a displays the effect of mass ratio (β) on the flutter boundaries of cantilever viscoelastic CNT conveying flow for $\mu = 0.1$, and $\alpha = 0.01$. In this figure, by increasing the mass ratio, the dimensionless critical speed and its stability region increase. Also, by increasing the Knudsen number, the dimensionless critical speed decreases. Effect of the nonlocal parameter on flutter boundaries in the $Kn - u_{cr}$ plane are plotted in Fig. 8b. As it can be seen, by increasing the nonlocal parameter, the critical speed decreases. Therefore, the stability regions decrease and the system become more unstable. This figure is shown for different nonlocal parameters $\mu = 0, 0.05, 0.1, 0.15$, With $\beta = 0.1$, and $\alpha = 0.01$. Fig. 8c indicates the effect of the structural damping α on the stability map in $Kn - u_{cr}$ plane for $\beta = 0.5$ and $\mu = 0.1$. The decrement of the dimensionless flutter speed arises from influence of both structural damping and Knudsen parameter.

As shown in Fig. 8, the mass ratio, nonlocal parameter and structural damping have significant effects on the stability region in the $Kn - u_{cr}$ plane for $0.0001 < Kn < 1$. Also, for $Kn > 1$, the mass ratio, nonlocal parameter and structural damping are not more significant.

It can be seen that for values of continuum flow regime ($10^{-4} < Kn < 10^{-2}$), the Knudsen number has no noticeable effect on the stability region and u_{cr} becomes almost constant vs. Kn, but effects of other parameters under investigation are still important. For slip flow regime ($10^{-2} < Kn < 10^{-1}$), effects of Kn, the mass ratio β, nonlocal parameter μ and structural damping α are noticeable on the stability region of CNT system. Hence, flutter boundaries are significantly influenced by the mass ratio, structural damping and nonlocal parameter of the slip flow regime and their effects cannot be ignored on the stability characteristics of the CNT. For transition flow regime ($10 < Kn$), the effect of Kn was remarkable on flutter boundaries and effects of other parameters could be ignored. However, for $Kn > 1$ the critical flow velocity tends to vanish and the effects of expected influential parameters on the critical flow velocity become faint. In the other words, influence of other parameters is reduced significantly after $Kn = 1$ and increasing the Knudsen number decreases the critical flow velocity considerably.

5. Conclusions

In this study, the dimensionless natural frequency and flutter boundaries for cantilever viscoelastic CNT conveying fluid are theoretically addressed. Nonlocal governing equation of motion and corresponding boundary conditions were derived by using Hamilton principle. Extended Galerkin method is adopted to obtain the numerical solutions to the model. Effects of structural damping, nonlocal parameter and Knudsen number on the eigenvalues and flutter boundaries of cantilever CNT are demonstrated. Our results indicate that the dimensionless critical speed decreases with increasing the structural damping and Knudsen number. It has shown that, however the eigenvalues are not very sensitive to the change of structural damping and Knudsen number, but these parameters play an important role in the flutter boundaries and stability region of cantilever CNT conveying fluid.

References

[1] R.W. Gregory, M.P. Paidoussis, Soc Proc. Royal. Lond. A 293 (1966) 512–527.
[2] M. Hosseini, S.A. Fazelzadeh, Int. J. Struct. Stab. Dyn 11 (2011) 513–534.
[3] D. Yu, M.P. Païdoussis, H. Shen, L. Wang, J. Appl. Mech 81 (2013). 011008-011008.
[4] B.-J. Ryu, S.-U. Ryu, G.-H. Kim, K.-B. Yim, KSME Int. J. 18 (2004) 2148–2157.
[5] S.-U. Ryu, Y. Sugiyama, B.-J. Ryu, Comput. Struct. 80 (2002) 1231–1241.
[6] V.M. Vassilev, P.A. Djondjorov, J. Sound Vib. 297 (2006) 414–419.
[7] X. Yang, T. Yang, J. Jin, Acta Mech. Solida Sin. 20 (2007) 350–356.
[8] X.-H. Yan, Q.-S. Yang, Comput. Mater. Sci. 98 (2015) 333–339.
[9] M. Eftekhari, S. Mohammadi, A.R. Khoei, Comput. Mater. Sci. 79 (2013) 736–744.
[10] I. Elishakoff, D. Pentaras, J. Sound Vib. 322 (2009) 652–664.
[11] M. Zidour, K.H. Benrahou, A. Semmah, M. Naceri, H.A. Belhadj, K. Bakhti, A. Tounsi, Comput. Mater. Sci. 51 (2012) 252–260.
[12] J. Yoon, C.Q. Ru, A. Mioduchowski, Compos. Sci. Technol. 65 (2005) 1326–1336.
[13] C.N.R. Rao, A.K. Cheetham, J. Mater. Chem. 11 (2001) 2887–2894.
[14] C. Li, L. Chen, J.P. Shen, J. Mech. 31 (2015) 7–19.
[15] G. Hummer, J.C. Rasaiah, J.P. Noworyta, Nature 414 (2001) 188–190.
[16] J. Yoon, C.Q. Ru, A. Mioduchowski, Int. J. Solids Struct. 43 (2006) 3337–3349.
[17] L. Wang, Physica E 41 (2009) 1835–1840.
[18] K. Yun, J. Choi, S.-K. Kim, O. Song, J. Mech. Sci. Technol. 26 (2012) 3911–3920.
[19] E. Ghavanloo, S.A. Fazelzadeh, Physica E 44 (2011) 17–24.
[20] Q. Wang, K.M. Liew, Phys. Lett. A 363 (2007) 236–242.
[21] M. Mirramezani, H.R. Mirdamadi, M. Ghayour, Comput. Mater. Sci. 77 (2013) 161–171.
[22] L. Wang, Comput. Mater. Sci. 49 (2010) 761–766.
[23] L. Wang, Comput. Mater. Sci. 45 (2009) 584–588.
[24] W. Xia, L. Wang, Comput. Mater. Sci. 49 (2010) 99–103.
[25] Y. Zhen, B. Fang, Comput. Mater. Sci. 49 (2010) 276–282.
[26] L. Wang, Q. Ni, Comput. Mater. Sci. 43 (2008) 399–402.
[27] A. Ghorbanpour, S. Arani, P. Amir, M. Dashti, Comput. Mater. Sci. 86 (2014) 144–154.
[28] V. Rashidi, H.R. Mirdamadi, E. Shirani, Comput. Mater. Sci. 51 (2012) 347–352.
[29] M. Mirramezani, H. Mirdamadi, Arch. Appl. Mech. 82 (2012) 879–890.
[30] A. Ghorbanpour Arani, M.Sh. Zarei, Ain Shams Eng. J. (2015).
[31] M. Hosseini, M. Sadeghi-Goughari, S. Atashipour, M. Eftekhari, Archiv. Mech. 66 (2014) 217–244.
[32] M. Sadeghi-Goughari, M. Hosseini, J. Mech. Sci. Technol. 29 (2015) 723–732.
[33] M.P. Paidoussis, Fluid-structure Interactions: Slender Structures and Axial Flow, Academic Press, 1998.
[34] G. Karniadakis, A. Beskok, N. Aluru, Microflows and Nanoflows Fundamentals and Simulation, Springer Science & Business Media, 2006.
[35] A.D. Drozdov, Viscoelastic Structures: Mechanics of Growth and Aging, Academic Press, 1998.
[36] P. Soltani, M.M. Taherian, A. Farshidianfar, J. Phys D: Appl. Phys 43 (2010) 425401.
[37] Q. Ni, Z.L. Zhang, L. Wang, Appl. Math. Comput. 217 (2011) 7028–7038.